Resonant photoemission in transition-metal chlorides

A. Kakizaki, K. Sugeno, and T. Ishii
Institute of Materials Science, University of Tsukuba, Sakura-mura, Ibaraki 305, Japan

H. Sugawara and I. Nagakura
Faculty of Education, Gunma University, Maebashi 371, Japan

S. Shin
Institute for Solid State Physics, University of Tokyo, Roppongi, Tokyo 106, Japan
(Received 31 January 1983)

In the chlorides of Ni, Co, Fe, and Mn, the resonance between the excitations of valence electrons and the $3p$ electrons of the metal ions is observed over the whole parts of the valence-band spectra including ligand-derived bands as well as satellites. The trend of the systematic change in satellite—to—main-band separations in going from $NiCl_2$ to $MnCl_2$ is opposite to that in the energies of charge-transfer excitons, and this is discussed in connection with the electron-shakedown mechanism of the hole-induced covalency. Excitation spectra consist of two or three overlapping bands approximately with Fano line shapes. The q value characterizing a Fano line shape is larger for satellites and ligand-derived bands than for the $3d$ bands of the metal ions. The resonant enhancements of the ionization cross sections of the main bands increase from $NiCl_2$ to $MnCl_2$. These aspects are interpreted in terms of the hybridization of the $3d$ orbitals of the metal ions and the $3p$ orbitals of the ligand ion. The ordinary $M_{2,3}VV$ super-Coster-Kronig bands are very weak.

I. INTRODUCTION

Resonant photoemission is a phenomenon in which the ionization cross section of an outer-shell electron enhances as the excitation energy exceeds the threshold of an inner-shell excitation and one of well-investigated recent topics in vacuum-ultraviolet radiation physics. It was first observed in metallic Ni (Ref. 1) and then in cerium pentaphosphate.[2] For rare-earth ions this phenomenon is understood as being due to a kind of configuration interaction in which a discrete transition from $4d^{10}4f^n$ to $4d^9 4f^{n+1}$ is mixed with a continuous transition to $4d^{10}4f^{n-1}\epsilon l$ and the excitation spectrum has a line shape of the Fano type.[3] The resonant enhancement of the ionization cross section of the $4f$ electron in a rare-earth element was used to investigate the valence fluctuation[4] rather than the resonance effect itself.[5]

In transition metals the resonance occurs at excitation energies near the $3p$ threshold; $3d$ outer-shell electrons involved in the resonance are itinerant and not so localized as $4f$ electrons in a rare-earth metal, and, therefore, the investigation of the resonant photoemission of a transition metal is theoretically quite interesting. In metallic Ni the resonant enhancement of the intensity of the main $3d$ band is not large[6] but a band located about 6 eV below the Fermi edge is appreciably enhanced on resonance.[6,7] Since this resonantly enhanced band appeared to be a satellite,[8,9] a lot of theoretical investigations[10–14] have been reported concerning the origin of the satellite and its contribution to the resonance process. The current understanding of the origin of the satellite in metallic Ni is the formation of the two-hole bound state where the scattering of conduction electrons by the pair hole potential is important. The $3p$-$3d$ resonance is also observed in transition metals other than Ni.[15,16] The resonance in the main $3d$ band is ascribed to the autoionization of a $3d$ electron through the super-Coster-Kronig decay of a photoproduced $3p$ hole.[11] So far, investigations have been concentrated on conductors,[1,6,7,11–18] especially on Ni and Cu with less than one $3d$ hole in the ground state, and only a few works have been reported on insulators[19–23] or materials of many-hole systems.[15–18]

In this report, we describe the extreme ultraviolet photoemission of the valence electrons of transition-metal chlorides in which $3d$ electrons are quite localized. Since no conduction electron is present, the screening of the hole potential is not important, and the many-electron effect caused by a photoproduced hole may be different from the case of a conductor.

II. EXPERIMENTAL PROCEDURE

Measurements were carried out at room temperature using synchrotron radiation from a 0.4-GeV electron storage ring at the Synchrotron Radiation Laboratory of the Institute for Solid State Physics, the University of Tokyo. A double-stage cylindrical mirror analyzer was used for photoelectron energy analyses. Synchrotron radiation, as excitation light, was monochromatized with a monochromator of a modified Rowland-mount type. Since the energy analyses were made by varying the voltage applied to analyzer electrodes, the kinetic energies of photoelectrons passing through the analyzer varied according to the applied voltage, and as a result the resolution varied with the excitation energy. Instead, no throughput correction in the retardation stage was necessary since the retardation voltage was fixed constant. The overall resolution was 0.4 eV at a 60-eV excitation. The ordinates for energy-

distribution curves presented in the following are indicated in relative scales, but photoelectron intensities shown there are normalized to the incident photon flux so that the spectra for different excitation energies may be compared directly with each other. The detailed procedure for the normalization, i.e., the correction for the throughput of the monochromator and for the ring current, is described elsewhere.[16] Since no reliable method to determine the location of the Fermi level of an insulator was found, the abscissas for the energy-distribution curves represent relative binding energies, the zeros of which are somewhat appropriate and do not necessarily correspond to the location of the Fermi level.

The samples were thin films of $NiCl_2$, $CoCl_2$, $FeCl_2$, and $MnCl_2$ prepared by evaporation. Since these materials are hygroscopic, they were baked in vacuum for a long time before they were used as starting materials for evaporation. The substrates were Au films vacuum-deposited on a stainless-steel plate. Sample thicknesses were controlled using a thickness monitor of a quartz-oscillator type. This was necessary for obtaining a thin film for which the charge-up effect was negligible. The pressure around samples during the measurements was about 5×10^{-10} Torr.

III. EXPERIMENTAL RESULTS

Energy-distribution curves for various excitation energies are shown in Figs. 1—4, illustrating some typical variations in spectral profiles. The line shapes agree with those reported previously by Ishii *et al.*[24] The spectra by excitations near the $3p$ thresholds of the metal ions, where the spectral profiles change abruptly, are shown in a smaller interval of excitation energy. In other excitation-energy regions, the change in the spectral profile occurs gradually. A detailed comparison of the energy-distribution curves at smaller intervals of excitation energies indicates that slight shifts in the locations of some structures occur at resonance, although they are not clear in Figs. 1—4. Fine structures are smeared at high excitation energies. Since the instrumental energy resolution at 120 eV is half as large as that at 60 eV, the smearing of fine structures appears more than that expected from the lowering of the instrumental resolution. Therefore, the intrinsic broadening such as the lifetime effect may be at least as large as the instrumental energy width.

Drastic changes in the spectral profile occur in the excitation-energy region below 35 eV and near the $3p$ threshold. Such changes are brought about by different intensity changes in different structures in the spectra, i.e., by different changes in the ionization cross sections of dif-

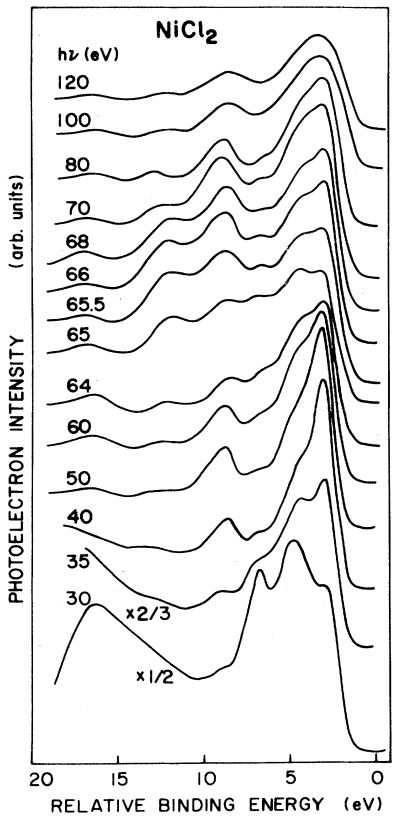

FIG. 1. Representative photoelectron energy-distribution curves for the valence-shell electrons in $NiCl_2$. Excitation energies are also shown. Original curves for 30- and 35-eV excitations are scaled by the factors shown.

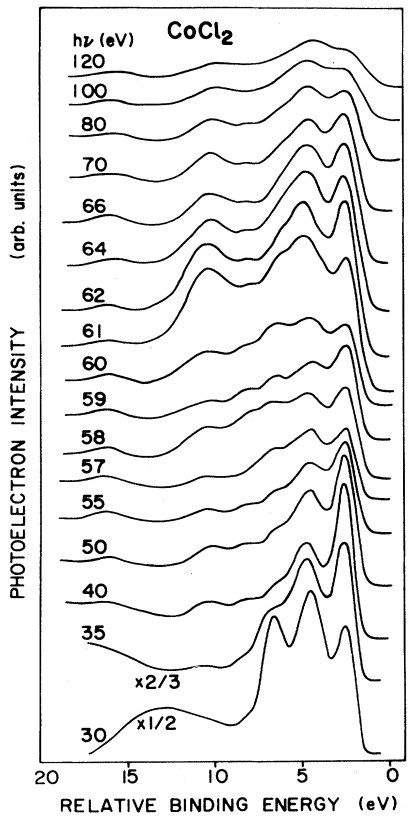

FIG. 2. Representative photoelectron energy-distribution curves for the valence-shell electrons in $CoCl_2$. Notations are the same as those in Fig. 1.

ferent component bands. The changes found below 35 eV are ascribed to the simple changes in the partial densities of states in the continuum states[25]; the intensity of the ϵf partial wave, when combining with the $3d$ states, increases with excitation energy in this region, making the components arising from the ligand $3p$ partial density of states apparently more prominent in the energy-distribution curves for excitations below 35 eV. The photoemission intensities decrease appreciably as the excitation energy increases from 30 to 40 eV. This may be ascribed to the decrease in the escape depth of the photoelectron. The change in the shape of a photoelectron spectrum with excitation energy near the $3p$ threshold of the metal ion is due to the resonance between the $3p$ inner-shell excitation and the valence-shell excitation.

Ishii *et al.*[24] interpreted their results obtained at only three different excitation energies in terms of the multiplet levels of $3d$ electrons of a transition-metal ion in the ligand field of a cluster ion as $(M\mathrm{Cl}_6)^{4-}$, M standing for a transition-metal element. Their interpretation is that the observed spectral features are incorporated by groups of multiplet lines broadened to some extent: a group forms a feature. Our basic interpretation of the spectral features is the same as theirs except that the importance of the effect of hybridization will be emphasized later in this work.

In Fig. 5, the ultraviolet photoelectron spectroscopy (UPS) spectra obtained here are compared with the x-ray photoelectron spectroscopy (XPS) $2p_{3/2}$ spectra of the transition-metal ions measured by Okusawa.[26] The structures in the UPS spectra are designated with capital letters. Among the various UPS spectra observed here, ones with the highest D peaks are chosen for the comparison. According to Ishii *et al.*,[24] the A_i ($i=1$, 2, and 3) structures are caused by the $3d$ multiplets and the B structure originates in the $3p$ states of the chlorine ion. The XPS $2p_{3/2}$ spectra are placed in Fig. 5 so that the centers of gravity of the main peaks align to those of the A_i structures in the UPS spectra. The XPS $2p_{3/2}$ spectra show weak composite structures and apparent broadening owing to the multiplet splitting arising from the coupling between $3d$ electrons and a photoproduced $2p$ hole, and to the electron transfer between molecular ions.[27] In the comparison between the UPS and XPS spectra in Fig. 5, only the separations of the C and D structures from the centers of gravity of the A bands are of interest since the origins of other fine structures are different between the UPS and the XPS spectra.

The C structure in $NiCl_2$ and the D structures in other chlorides were assigned to multielectron satellites previously.[24] Figure 5 indicates that the C and D structures have a good correspondence to the satellites of the XPS $2p_{3/2}$ lines appearing on the high-binding-energy sides of the main lines. The satellite of the $2p_{3/2}$ line has been ascribed to the increase in covalency caused by a photopro-

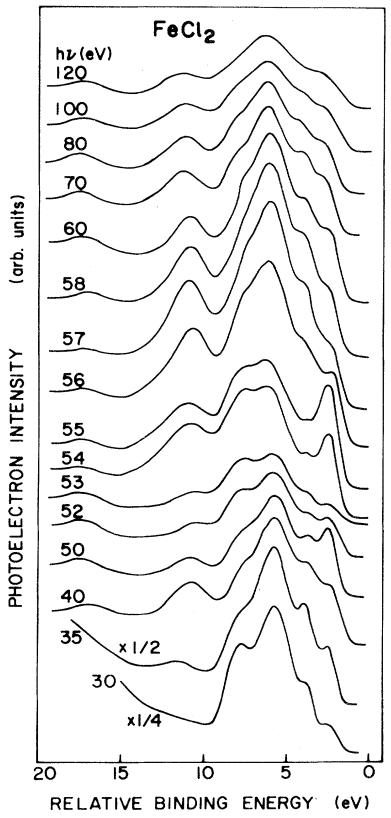

FIG. 3. Representative photoelectron energy-distribution curves for the valence-shell electrons in $FeCl_2$. Notations are the same as those in Fig. 1.

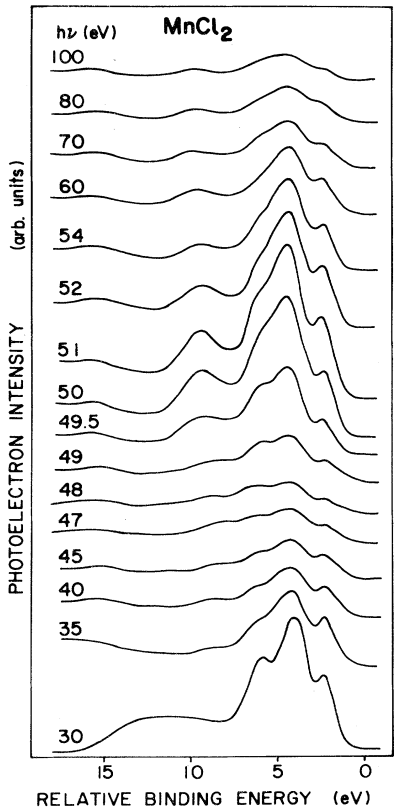

FIG. 4. Representative photoelectron energy-distribution curves for the valence-shell electrons in $MnCl_2$. Notations are the same as those in Fig. 1.

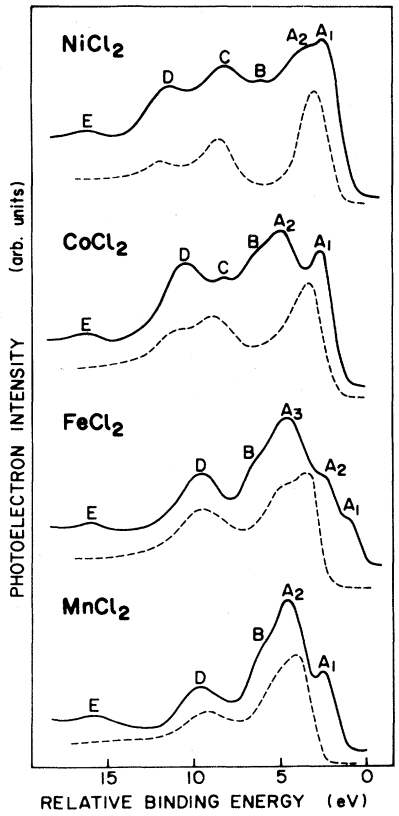

FIG. 5. Valence-shell photoelectron spectra on resonance (solid line) as compared with the XPS $2p_{3/2}$ spectra (dashed line) from Ref. 23. Main structures are designated by capital letters. Excitation energies for the valence-shell spectra are 66 eV in $NiCl_2$, 61 eV in $CoCl_2$, 57 eV in $FeCl_2$, and 51 eV in $MnCl_2$, respectively.

duced hole.[28] The process is essentially the redistribution of charge expressed by the change in the hybridization. From another point of view, it resembles the shake-up transfer of charge from ligand ions to a metal ion, and may also be treated as the electron shakedown incorporated by a large relaxation due to the hole potential.[29] The good correspondence of the high-binding-energy structures between the valence-band spectra and the $2p_{3/2}$ spectra appears to show that the satellites in the valence-band spectra are also caused by the hole-induced covalency.[28,29] In this case, however, the potential to induce such an effect is produced by a hole in the $3d$ state instead of the $2p$ state. Such a similarity in the satellite feature between the valence-band spectrum and the $2p_{3/2}$ spectrum was also found in metallic Ni.[8,9]

It is interesting to compare the separations between the satellites and the main bands with the energies of the charge-transfer excitons found in the fundamental optical-absorption spectra.[30] The satellite—to—main-band separations and the energies of the charge-transfer excitons are tabulated in Table I. Since the main $3d$ bands have composite structures, the satellite—to—main-band separations were estimated as the distances from the centers of gravity of all the A_i structures. Three bands are

TABLE I. Satellite—to—main-band separations and the energies of the charge-transfer excitons. Values in the parentheses are from the XPS data of Ref. 26. Centers of gravity are used as the main $3d$-band locations. All units are eV. (PES designates photoelectron spectroscopy.)

		$NiCl_2$	$CoCl_2$	$FeCl_2$	$MnCl_2$
PES-satellite	C	5.5 (5.4)	5.0 (5.2)		
	D	8.8 (8.6)	7.1 (7.3)	6.0 (5.6)	5.7 (5.3)
Exciton	A^*		4.3	5.7	7.3
	B^*	4.7	5.8	6.6	8.9
	C^*	6.4	6.9	7.4	8.0

assigned to the charge-transfer excitons in the fundamental absorption spectra in the ultraviolet region. They are referred to as A^*, B^*, and C^* here. The A^* band originates in the transition from the ligand orbital to the t_{2g} orbital of the metal ion and the B^* band in the transition to the e_g orbital. Table I shows that the satellite—to—main-band separation decreases in going from $NiCl_2$ to $MnCl_2$, whereas the energy of the charge-transfer exciton increases in this order. In $NiCl_2$, the satellite—to—main-band separation is larger than the energy of the charge-transfer exciton, while the former is smaller than the latter in $MnCl_2$.

The E structure is common in all the chlorides observed here. This peak shows a very weak resonance. These characteristics, along with the comparison of the binding energies with those in a standard table of the atomic energy levels,[31] suggest that the E peak arises from the Cl $3s$ level.

Figures 6—9 show the excitation spectra defined as the excitation-energy dependences of the intensities at various structures in the energy-distribution curves. Each curve denoted by a capital letter indicates the intensity variation of the feature denoted by the same capital letter in the energy-distribution curves. The partial-yield spectra are also shown for comparison. They are a kind of constant final-state spectra representing the plots of intensity of the photoelectrons with a constant kinetic energy of 8 eV versus the photon energy. Around 8 eV, only inelastically scattered electrons contribute to the spectra and their intensities are quite strong. It is well known that the photoelectric yield spectrum has a profile similar to the optical-absorption spectrum.[32] The partial yield spectra shown in Figs. 6—9 agree well with the optical-absorption data obtained by Nakai *et al.*[33]; the resolution is somewhat better in the present data. Main structures in the excitation spectra are denoted by Greek letters: α, β, and γ.

The intensities in the spectra shown in Figs. 6—9 were obtained just as heights of structures in the energy-distribution curves, not as the integrated intensities. The heights were estimated after subtracting smooth backgrounds caused by inelastically scattered electrons. Because of the overlap of adjacent structures, the obtained excitation spectra are affected by some averaging. However, the decomposition of the overlapping bands cannot be made without an ambiguity; the ambiguity introduced by

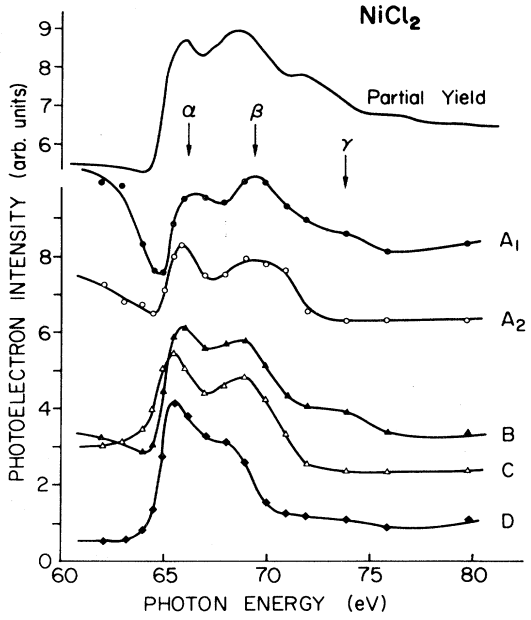

FIG. 6. Excitation spectra defined as the plots of photoelectron intensities vs excitation energies for the main structures in the energy-distribution curves for the valence-shell electrons in $NiCl_2$. Capital letters designate the structures in the energy-distribution curves. Greek letters designate the main structures in the excitation spectra. Partial-yield spectrum defined as the intensity of photoelectrons with a kinetic energy of 8 eV vs excitation energies is shown by the uppermost curve.

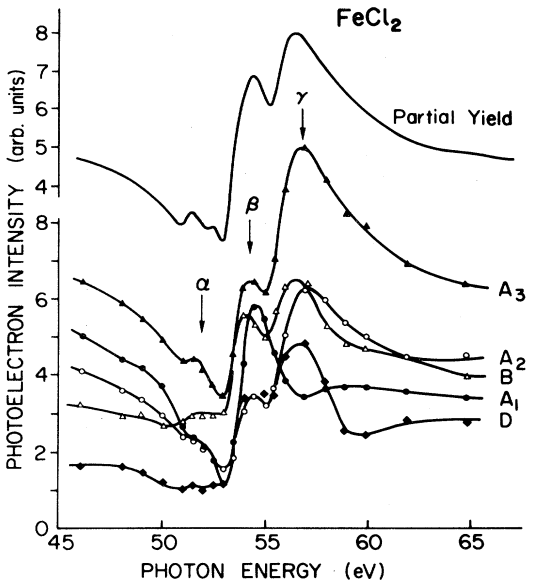

FIG. 8. Excitation spectra for the main structures in the energy-distribution curves in $FeCl_2$. Notations are the same as those in Fig. 6.

the decomposition may be as large as the error due to the averaging.

Some of the excitation spectra do not have all of the α, β, and γ peaks. For example, the A_1 curve in $FeCl_2$ has only the β peak, but the D curve has the γ peak as its major resonance peak and the β peak is weak; in $CoCl_2$ only the A_2 and B curves have the γ peak. Such an aspect suggests that the effect of the overlap of neighboring struc-

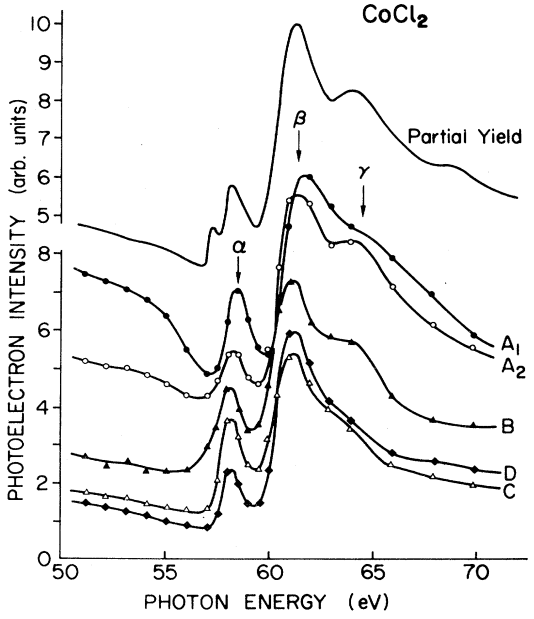

FIG. 7. Excitation spectra for the main structures in the energy-distribution curves in $CoCl_2$. Notations are the same as those in Fig. 6.

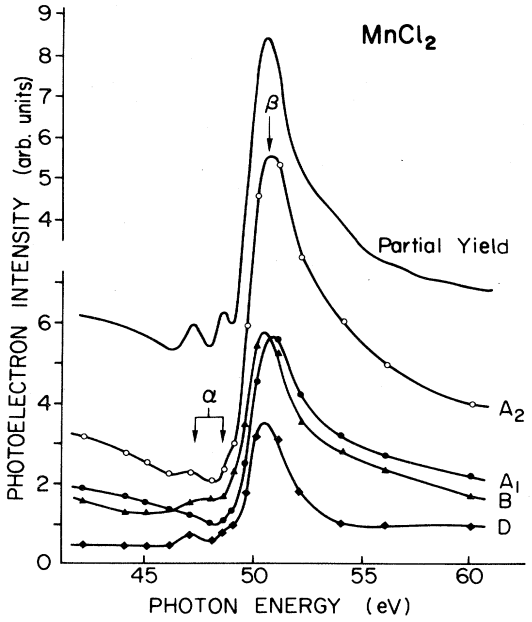

FIG. 9. Excitation spectra for the main structures in the energy-distribution curves in $MnCl_2$. Notations are the same as those in Fig. 6.

tures in the energy-distribution curves is not so serious as to make the plots shown in Figs. 6—9 meaningless; in $NiCl_2$ the A_1 structure overlaps the A_2 structure to some extent but the A_1 excitation spectrum is clearly different from the A_2 excitation spectrum as is obvious in Fig. 6. Thus, we conclude that the spectra shown in Figs. 6—9 may tolerate a qualitative discussion made later in this work.

The spectral features in the yield spectra in Figs. 6—9 are caused by the transitions of the $3p$ electrons of the metal ions. The excitation spectra show the corresponding features and this represents the resonance.

All of the A_i curves show antiresonant features with dips near the $3p$ thresholds. The B curves have asymmetric line shapes with almost no distinct dip structure. Concerning the occurrence of a dip profile, the D curves are intermediate between the A_i curves and the B curves. The C curves are somewhat similar to the D curves. According to Davis and Feldkamp,[11] the line shape of an excitation spectrum may be represented as

$$N(\epsilon)=A(\epsilon)+\sum_j K_j f_j(\epsilon) . \tag{1}$$

Here, ϵ represents the normalized excitation energy and the first term is the background which varies slowly and smoothly with the excitation energy. The second term is the resonant part and $f_j(\epsilon)$ represents a resonance line shape; K_j is an amplitude. The subscript j distinguishes different resonance energies. Generally, $f_j(\epsilon)$ is not expressed as a simple analytical form, but it is suggested[11] that $f_j(\epsilon)$ is approximated by a Fano line shape in a simplified system. In spite of the fact that many continuous and discrete states are involved in the final-state configuration[11—14] owing to the multiplet splitting,[24,26—28,34] and that an observed spectrum should be given as the resulting superposition, a simplified analysis works well actually in many cases, and we analyze the excitation spectra obtained here using Eq. (1) with a Fano line shape for $f_j(\epsilon)$ as

$$f_j(\epsilon)=\frac{(\epsilon+q)^2}{\epsilon^2+1} , \qquad \epsilon=(h\nu-h\nu_j)/\Gamma_j . \tag{2}$$

Here $h\nu_j$ is a resonance energy and Γ_j is a quantity like the self-energy of the resonance. We distinguish the features labeled with α, β, and γ by different $h\nu_j$ and Γ_j. A common q value is assumed[11] for all features in an excitation spectrum. An example of such a fitting is shown in Fig. 10. Figure 10 is for the A_3 curve of $FeCl_3$. Curve 2 is obtained by subtracting smooth backgrounds illustrated by a chain line from the measured spectrum shown as curve 1. Points in curve 2 illustrated by open circles are decomposed into three components illustrated by dots and triangles. Fitted Fano lines are shown by thin curves denoted as 3 and 4. The curve for the α structure, given by a broken line, is obtained by just connecting the points. In many cases, the analysis of the α structure was not made, because the intensity is low and an appreciable ambiguity may be introduced. In the case of $FeCl_2$, the feature above the dip at 57 eV in the A_1 curve as well as the broad feature above the dip at 59 eV in the D curve was neglected.

The Fano parameters obtained in this way are tabulated

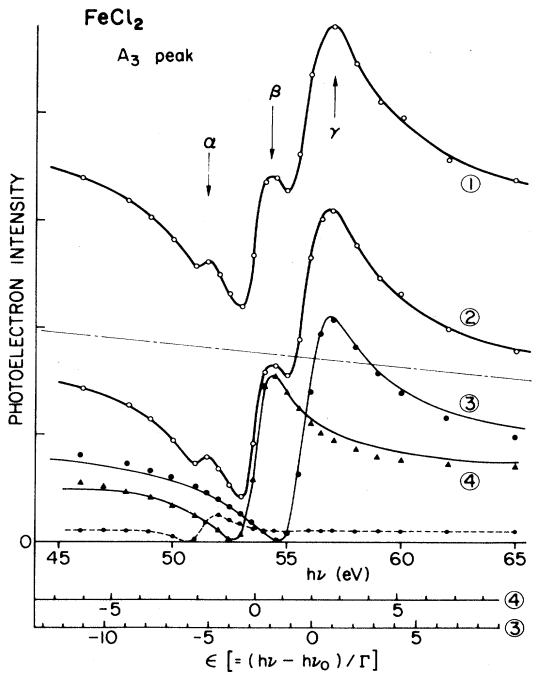

FIG. 10. Decomposition of the A_3 excitation spectrum in $FeCl_2$. Curve 1 is the spectrum as measured. Curve 2 is obtained by subtracting the background illustrated by a chain line. Dots and triangles are obtained by decomposing the points in curve 2. Curves 3 and 4 represent the spectra given by the Fano formula. Broken curve is obtained by just connecting the points. Three different abscissas represent the photon energy $h\nu$ and the normalized excitation energies ϵ for curves 3 and 4. Main structures in the excitation spectrum are designated α, β, and γ.

in Table II. Table II indicates that q values are larger for the B structures than for the A_i structures. According to the assignment of the structures already mentioned, this means that the q value is larger for the band originating mainly in the Cl $3p$ state than for that originating mainly in the $3d$ state of the transition-metal ion.

In $NiCl_2$ the resonant enhancement of the main band is not strong, and the resonance is recognized only as a dip in the excitation spectrum. Equation (2) predicts that the height of the resonantly enhanced peak is small as compared with the depth of the antiresonance dip for a small q value, and this is the case for the A_1 structure in $NiCl_2$. The peak-to-peak intensity of a resonance band is also dependent on the amplitude K_j. In order to investigate such a situation in more detail, the resonant enhancement factors defined as

$$R=\frac{K_j(q^2+1)}{A+K_j} \tag{3}$$

are calculated and tabulated in Table III. Here, it should be remarked that $A+K_j f(\infty)=A+K_j$ and the maximum resonant enhancement is $K_j(q^2+1)$. In evaluating R, the magnitudes of the numerator were obtained as the peak-to-peak heights of the decomposed bands used in the estimation of the Fano parameters. Selected j is α for

TABLE II. Parameters characterizing the Fano line shape obtained by data fitting. Greek letters stand for the structures in the excitation spectra. Capital letters stand for the structure in the energy-distribution curves and distinguish the excitation spectra.

		$NiCl_2$			$CoCl_2$			$FeCl_2$			$MnCl_2$		
		q	Γ	$h\nu_0$	q	Γ	$h\nu_0$	q	Γ	$h\nu_0$	q	Γ	$h\nu_0$
A_1	α	0.83	0.86	65.5	1.3	0.81	57.9						
	β	0.83	1.3	68.2	1.3	1.2	61.1	1.0	0.90	53.7	2.1	1.2	50.2
A_2	α	1.8	0.72	65.6	1.7	0.83	57.8						
	β	1.8	1.4	68.9	1.7	1.2	60.9	1.0	0.85	53.7	1.9	1.2	50.1
	γ				1.7	1.2	64.0	1.0	1.4	56.0			
A_3	β							1.2	0.80	53.6			
	γ							1.2	1.2	56.0			
B	α	3.2	1.1	65.2	2.3	0.92	57.8						
	β	3.2	1.3	68.8	2.3	1.2	60.7	2.1	0.85	53.6	3.0	1.1	50.1
	γ				2.3	1.0	63.7	2.1	1.1	56.2			
C	α	3.0	0.82	65.7	2.6	0.65	58.0						
	β	3.0	1.3	68.6	2.6	1.1	60.9						
D	α	4.0	0.79	65.4	2.2	0.55	57.9						
	β	4.0	0.88	68.0	2.2	1.1	60.7	1.8	0.91	53.9	3.2	0.86	50.2
	γ							1.8	0.96	56.2			

$NiCl_2$, β for $CoCl_2$ and $MnCl_2$, and γ for $FeCl_2$, and the value of A was estimated at the energy of the peak of the corresponding j component curve. The magnitude of R represents the strength of the resonance and the selected j corresponds to the structure giving the largest R value in each material.

Table III shows that the resonance is stronger in the satellite than in the main band in a given material. The resonant enhancement of the main band is the strongest in $MnCl_2$ in all the chlorides measured here. In $NiCl_2$ the resonance in the A_i structures is weaker than that in the B structure. This tendency is the same in $CoCl_2$ but the magnitude is not so large as in $NiCl_2$. The situation is opposite in $FeCl_2$ and $MnCl_2$. The resonance in the A_i structures tends to be larger in the order from $NiCl_2$ to $MnCl_2$.

In the chlorides observed here, the ordinary $M_{2,3}VV$ super-Coster-Kronig lines are very weak. Ordinary Auger or super-Coster-Kronig electrons have a constant kinetic energy, and thus the corresponding spectral lines in a photoelectron spectrum plotted against the binding energy shift by an amount equal to the change of the photon energy as the photon energy is changed. In the chlorides observed here, such a peak was not found even for photon energies near the $3p$ thresholds of the metal ions. This situation is quite contrasted to the cases of materials with metallic conductivities.[1,2,6,16–18] For photon energies far from the resonance region the ionization cross section of the $3p$ electron of the transition-metal ion is small. Actually, the integrated intensity of the $3p$ inner-shell line by an excitation at 120 eV is about 15% of that of the valence-band intensity in $MnCl_2$, 12% in $FeCl_2$, 7% in $CoCl_2$, and 6% in $NiCl_2$. The relative integrated intensities of the ordinary super-Coster-Kronig bands cannot be larger than those fractional intensities. Since the super-Coster-Kronig bands are broad, they are not easily observable if they are weak. A weak $3p$ inner-shell line was found in the case of Mn vapor.[35] The super-Coster-Kronig lines appear also very weak in Ni-phthalocyanine[19] and Cu-phthalocyanine.[20]

TABLE III. Resonant enhancement factors R.

	$NiCl_2$	$CoCl_2$	$FeCl_2$	$MnCl_2$
A_1	0.39	0.90	1.7	1.9
A_2	0.33	1.2	1.4	5.2
A_3			0.90	
B	0.94	1.8	1.1	3.8
C	1.2	2.7		
D	7.8	2.9	2.5	6.4

IV. DISCUSSION

In the previous analysis[24] the hybridization between the $3p$ orbitals of chlorine and the $3d$ orbitals of the transition metal was not taken into account explicitly. There, the effect of the hybridization may be regarded as being renormalized implicitly and incompletely into the selected spectroscopic and crystal-field parameters. In the present measurements, it has been found that all the structures in the valence-band spectra including the B structure show resonant behaviors.

If the state responsible for the B structure arises only from the $3p$ orbitals of chlorine localized to a chlorine-ion site, their coupling with the $3p$ hole state of a transition-metal ion is small and no resonance is expected to occur in this structure. A similar situation is actually the case in the E structure assigned to the $3s$ level of chlorine. The resonant behavior in the B structure suggests that the hybridization between the $3p$ orbitals of the chlorine ion and the $3d$ orbitals of the transition-metal ion is not negligible; the resonance may be caused by the $3d$ orbitals mixed in the B states.

The $3p$-$3d$ resonance has been found in the itinerant $3d$ states.[6,16,18] Theories suggest that the resonance is brought about by the amplitude of the $3d$ wave function at the site where the $3p$ inner-shell hole is produced. This is a situation similar to the hybridization in an ionic material. It is interesting to point out that there exist $3d$ materials, like transition-metal silicides,[18] in which the resonance is weak.

The spectra shown in Figs. 1—4 are not similar to the spectra of the gaseous materials.[36] The molecule of a transition-metal chloride in the gas phase is composed of a linear chain of atoms. The observed photoelectron spectra of various gaseous transition-metal chlorides are similar to each other, and the spectra are interpreted in terms of the simple molecular orbital levels of a linear molecule. The spectra of the solid-phase materials are different from each other as is obvious in Figs. 1—4. Perhaps the hybridization may be quite strong in a gaseous molecule and this obscures the intraionic electrostatic interaction to produce to multiplet structure responsible for some spectral features in a solid material.

Among the chlorides observed here, the trend of the material dependence of the satellite—to—main-band separation is opposite to that of the energy of the charge-transfer exciton. If the hole-induced covalency which is similar to the transfer of charge from the ligand ion to the metal ion is caused by the electron shake-up mechanism where the electron is promoted from the ligand level to an empty level of the metal ion, the trend of the satellite—to—main-band separation should be parallel to the trend of the energy of the charge-transfer exciton in contrast to the result observed here. If the hole-induced covalency is caused by the electron shake-down mechanism,[10,29] the situation may be reversed. In this mechanism, an unoccupied $3d$ level is pulled down by a large relaxation due to the potential of a photoproduced $3d$ hole. The resulting two bound holes attract an electron from a ligand ion to form a bound state. The extra energy to cause such a process is roughly equal to the intra-atomic Coulomb energy for the two bound holes minus the energy of the charge-transfer exciton. This extra energy varies as the material changes and the negative contribution of the energy of the charge-transfer exciton indicates a possibility of the trend of the satellite—to—main-band separation opposite to that of the charge-transfer exciton. According to this assignment, the locations of the main band and the satellite are reversed to the case of the electron shake up. However, this is a problem of definition, and we may refer to a band occurring at a lower binding energy as the main band. In a simplified model, the intermediate state of this shake-down process with two $3d$ holes should have the $3d^{n-1}$ configuration and the final state should have the $3d^n\hat{L}$ configuration, $\hat{L}$ representing the hole state of the ligand ion. The multiplet arising from the intermediate state is essentially the same as that for the main band considered previously.[24] Originally, the electron shake-down model is appropriate for a system with itinerant electrons like a metal. Thus, it is necessary to modify the theory so as to make it applicable to a localized electron system which we are concerned with, and this is a problem remaining to be solved.

Recently, Thuler *et al.*[23] observed that the valence-shell satellite of CuO at resonance is twice as intense as those in Cu and Cu_2O, and that the satellites in Cu and Cu_2O are not detectable by excitations far from resonance. They suggested that the satellite in a transition-metal oxide with the unfilled $3d$ shell is not due to the "ligand-to-metal charge transfer transition," but rather is due to the intra-d-shell monopole transition. According to their assignment, the satellite is one of the components of the $3d^{n-1}$ multiplet. However, such multiplets compose the main $3d$ bands in the transition-metal chlorides observed here.

That the q value is smaller for the band derived mainly from the $3d$ states of the metal ion than for the band derived mainly from the Cl $3p$ states may be explained qualitatively by the hybridization between the $3d$ state of the metal ion and the $3p$ state of the chlorine ion. According to Davis and Feldkamp[11] the q value is approximately given, in the most simplified case with no hybridization, as

$$q_0=\frac{\langle d\,|\,r\,|\,p\rangle}{\pi\langle p\epsilon l\,|\,e^2/r\,|\,dd\rangle\langle\epsilon l\,|\,r\,|\,d\rangle}\ . \tag{4}$$

Here, $|p\rangle$, $|d\rangle$, and $|\epsilon l\rangle$ are the basis functions representing the $3p$, $3d$, and continuum state of the metal ion, respectively. If the discrete state is postulated to be given by a simple hybridization of the $3d$ state of the metal ion and the $3p$ state of the chlorine ion as

$$\phi\sim\frac{1}{(a^2+b^2)^{1/2}}(a\,|\,d\rangle+b\,|\,L\rangle)\ ,$$

where $|L\rangle$ is the $3p$ orbital of chlorine, then a more rigorous formula for the q value [Eq. (2.30) in Ref. 11] suggests that $|d\rangle$ in Eq. (4) should be replaced by $a\,|\,d\rangle/(a^2+b^2)^{1/2}$ and the resulting q value may be given as

$$q=q_0(1+r)\ . \tag{5}$$

Here, $r\,(=b^2/a^2)$ represents the magnitude of the hybridization. In a more exact expression,[10,11] we must calculate the determinant describing the overlap between the ground state and the excited state of the many-electron system. Equation (5) predicts that q is near to q_0 for the state derived mainly from the $3d$ state of the metal ion since r is small for this state, and that q becomes large for the state derived mainly from the $3p$ state of chlorine since r is large in this case. These qualitatively explain a trend of the q values for the different structures in the energy-distribution curves.

As is obvious in Table II, the q value is larger for the satellite than for the main $3d$ band. The profiles of the excitation spectra of Cu-phthalocyanine[20] suggest that such a tendency exists also in this material. It was shown that the satellite in metallic Ni caused by the two-hole bound state has a resonance profile near to a Fano shape with a large q value,[11] and that the atomic Auger line has a symmetric resonance profile.[37] The result obtained here is qualitatively similar to the tendency found for the satellite of metallic Ni.[6] According to the model of the hole-induced covalency for the satellite, the hybridization is increased in the final state.[27] This leads to the increase in the value of r. The large q value of the satellite is explained by a large value of r due to the hybridization as in the case of the ligand-derived band.

Shin *et al.*[34] interpreted their photoabsorption data as being due to the multiplet lines arising from the interaction between an inner-shell hole and $3d$ electrons and broadened by the Fano effect. In the present analysis of the excitation spectra, the multiplet lines are treated as if they form a few bands, the widths of which are much narrower than the broadening caused by the Fano effect.

Recently, Davis[22] suggested that the magnitude of the resonance of the main $3d$ band is strongly dependent on the strength of the hybridization. In this theory, the basis function representing two holes localized only in the $3d$ state of the metal ion is responsible for the resonance, and all other basis functions contribute only to the part of the ionization cross section which does not resonate. As the hybridization becomes strong, the amplitude K_j representing the intensity of the resonant part becomes small and R becomes small. This theory predicts that the hybridization would be strong in $NiCl_2$ but weak in $MnCl_2$, since R is small in $NiCl_2$ and large in $MnCl_2$ as is obvious in Table III. However, this is against the trend of the q values shown in Table I; a larger hybridization leads to a larger q value. However, this is not a crucial difficulty. The magnitude of the q value is determined not only by the hybridization but also by the value of q_0 given in Eq. (4). Therefore, the magnitudes of the q values of *different materials* cannot be compared by the strength of the hybridization only. In a given material the relative magnitudes of the q values for the different structures in the energy-distribution curves are determined by the values of r in Eq. (5), and thus by the hybridization since q_0 is common in this case. The value of R, the strength of the resonance, is determined by the value of K_j/A, and thus by the hybridization. In the case of the satellite, the effect of the hybridization on the resonance strength may be different from the case of the main band. This is a problem remaining to be solved in the future.

Concerning Eq. (3), a spurious discrepancy exists: If $\langle p\epsilon l \mid e^2/r \mid dd \rangle$ approaches zero, q_0 approaches infinity according to Eq. (4); then R becomes infinite unless K_j is zero. This would lead to an absurd result that the resonance becomes strong when the interaction between the innershell hole and the outershell electron is weak. Thus, K_j should approach zero if $\langle p\epsilon l \mid e^2/r \mid dd \rangle$ approaches zero so that R remains finite. In a more rigorous treatment[11,14] of the photoemission intensity, it is shown that the resonance becomes weak if the interaction between the inner-shell hole and the outer-shell electron is weak. [For example, $D_k \rightarrow$ finite as $V_{kn}(E) \rightarrow 0$ in Eq. (2.29) in Ref. 11.]

The ordinary super-Coster-Kronig transition far from resonance is weak in the materials treated here. The initial state for an ordinary super-Coster-Kronig transition is a relaxed excited state with a relaxed inner-shell hole. In the case where the matrix element for the super-Coster-Kronig coupling becomes very large, the coupling of the direct excitation of the outer-shell electron with the super-Coster-Kronig transition becomes large enough to initiate the outer-shell transition before the formation of the relaxed state with a relaxed inner-shell hole and the ordinary super-Coster-Kronig transition does not occur. In the case of a conductor in which the ordinary super-Coster-Kronig transition is clearly observed,[1,5,6,15–18] an excited electron leaving an inner-shell hole is scattered by conduction electrons. If this scattering occurs very fast, the excited state that is to couple with the outer-shell excitation disappears in a very short time and the relaxed inner-shell hole state is produced. For excitation energies far above the resonance, the ionization cross section of the $3p$ electron is small, resulting in a weak super-Coster-Kronig band.

ACKNOWLEDGMENTS

The authors appreciate Dr. M. Okusawa for allowing them to use his XPS data prior to publication. One of the authors (T.I.) would like to thank Dr. L. C. Davis, Dr. B. Sonntag, Dr. A. Kotani, and Dr. F. Fujiwara for stimulating and helpful discussions. The support by the staff of Synchrotron Radiation Laboratory of the Institute for Solid State Physics, the University of Tokyo, is greatly acknowledged. The present work was partly supported by the Grant-in-Aid for Scientific Research from the Ministry of Education, Science and Culture, Japan, and by the Fund for the Special Science Project Research of the University of Tsukuba.

[1] C. Guillot, Y. Ballu, J. Paigne, J. Lecante, K. J. Jain, P. Thirty, R. Pinchaux, Y. Petroff, and L. M. Falicov, Phys. Rev. Lett. 39, 1632 (1977).

[2] W. Length, F. Lutz, J. Barth, G. Kalkoffen, and C. Kunz, Phys. Rev. Lett. 41, 1185 (1978).

[3] U. Fano, Phys. Rev. 124, 1866 (1961); Y. Toyozawa and A. Kotani, in *Synchrotron Radiation*, edited by C. Kunz (Springer, Berlin, 1979) Chap. 4, p. 196.

[4] H. Sugawara, A. Kakizaki, I. Nagakura, T. Ishii, T. Komatsubara, and T. Kasuya, J. Phys. Soc. Jpn. 51, 915 (1982), and references therein; J. M. Lawrence, J. W. Allen, S. -J. Oh, and I. Lindau, Phys. Rev. B 26, 2362 (1982), and references therein; D. J. Peterman, J. H. Weaver and M. Croft, Phys. Rev. B 25, 5530 (1982), and references therein.

[5] S.-J. Oh and S. Doniach, Phys. Rev. B 26, 1859 (1982); M. Iwan, E. E. Koch, and F. J. Himpsel, Phys. Rev. B 24, 613 (1981); B. Reihl, N. Martensson, D. E. Eastman, A. J. Arko, and O. Vogt, Phys. Rev. B 26, 1842 (1982).

[6] J. Barth, G. Kalkoffen, and C. Kunz, Phys. Lett. 74A, 360 (1979).

[7] M. Iwan, F. J. Himpsel, and D. E. Eastman, Phys. Rev. Lett. 43, 1829 (1979).

[8] S. Hüfner and G. K. Wertheim, Phys. Lett. 51A, 299 (1975).

[9] P. C. Kemeny and N. J. Shevchik, Solid State Commun. 17, 255 (1975).

[10] A. Kotani, J. Phys. Soc. Jpn. 46, 488 (1979).

[11] L. C. Davis and L. A. Feldkamp, Phys. Rev. B 23, 6239 (1981).

[12] S. M. Grivin and D. R. Penn, Phys. Rev. B 22, 4081 (1980); J. Appl. Phys. 52(3), 1650 (1981).

[13] A. Liebsch, Phys. Rev. B 23, 5025 (1981), and references therein.

[14]J. C. Parlebas, A. Kotani, and J. Kanamori, Solid State Commun. 41, 439 (1982); J. Phys. Soc. Jpn. 51, 124 (1982).
[15]J. Barth, F. Gerken, K. L. I. Kobayashi, J. H. Weaver, and B. Sonntag, J. Phys. C 13, 1369 (1980).
[16]H. Sugawara, A. Kakizaki, I. Nagakura, and T. Ishii, J. Phys. F 12, 2929 (1982).
[17]A. Kakizaki, H. Sugawara, I. Nagakura, and T. Ishii, J. Phys. Soc. Jpn. 49, 2183 (1980).
[18]A. Kakizaki, H. Sugawara, I. Nagakura, Y. Ishikawa, T. Komatsubara, and T. Ishii, J. Phys. Soc. Jpn. 51, 2597 (1982).
[19]M. Iwan and E. E. Koch, Solid State Commun. 31, 261 (1979).
[20]M. Iwan, E. E. Koch, T.-C. Chiang, D. E. Eastman, and F.-J. Himpsel, Solid State Commun. 34, 57 (1980).
[21]S.-J. Oh, I. Lindau, and J. C. Mikkelsen, Phys. Rev B 26, 4845 (1982).
[22]L. C. Davis, Phys. Rev. B 25, 2912 (1982).
[23]M. R. Thuler, R. L. Benbow, and Z. Hurych, Phys. Rev. B 26, 669 (1982).
[24]T. Ishii, S. Kono, S. Suzuki, I. Nagakura, T. Sagawa, R. Kato, M. Watanabe, and S. Sato, Phys. Rev. B 21, 4320 (1975).
[25]S. Hüfner, in *Photoemission in Solids II,* edited by L. Ley and M. Cardona (Springer, Berlin, 1979), Chap. 3, p. 173.
[26]M. Okusawa, thesis, Tohoku University, 1976 (unpublished).
[27]S. Asada and S. Sugano, J. Phys. C 11, 3911 (1978), and references therein.
[28]S. Asada and S. Sugano, J. Phys. Soc. Jpn. 41, 1291 (1976).
[29]A. Kotani and Y. Toyozawa, J. Phys. Soc. Jpn. 37, 563 (1974).
[30]Y. Sakisaka, T. Ishii, and T. Sagawa, J. Phys. Soc. Jpn. 36, 1365 (1974); T. Ishii, Y. Sakisaka, T. Matsukawa, S. Sato, and T. Sagawa, Solid State Commun. 13, 281 (1973).
[31]A. J. Bearden and A. F. Burr, Rev. Mod. Phys. 39, 125 (1967).
[32]C. Kunz, in *Photoemission in Solids II,* Ref. 25, Chap. 6, p. 322.
[33]S. Nakai, H. Nakamori, A. Tomita, K. Tsutsumi, H. Nakamura, and C. Sugiura, Phys. Rev. B 9, 1870 (1974).
[34]S. Shin, S. Suga, M. Taniguchi, H. Kanzaki, S. Shibuya, and T. Yamaguchi, J. Phys. Soc. Jpn. 51, 906 (1982).
[35]B. Sonntag (private communication).
[36]J. Berkowitz, D. G. Street, and A. Garritz, J. Chem. Phys. 70, 1305 (1979).
[37]Y. Yafet, Phys. Rev. B 21, 5023 (1980).